Human Threshold Model for Perceiving Changes in System Dynamics

Fu, Wei; van Paassen, M. M.; Mulder, Max

DOI
10.1109/THMS.2020.2989383

Publication date
2020

Document Version
Final published version

Published in
IEEE Transactions on Human-Machine Systems

Human Threshold Model for Perceiving Changes in System Dynamics

Wei Fu, M. M. van Paassen, *Senior Member, IEEE*, and Max Mulder, *Member, IEEE*

***Abstract*—Limitations of a haptic device can cause distortions of the force feedback it presents. Just-noticeable difference (JND) in system dynamics is important for creating transparent haptic interaction. Based on the previous work, this article presents a unified model that extends the existing JND rule. Our approach projects the JNDs in the mechanical properties of a second-order mass-spring-damper system onto the real and imaginary components of the system's frequency response function (FRF). We discuss the results of two experiments and show that the JNDs obtained for both the real and imaginary components can be expressed as *the same fraction* of, and thus are proportional to, the magnitude of the total system's FRF. Furthermore, the findings are generalized to cases where the system's dynamics order is different than two. What results is a unified model that accurately describes the threshold for changes in human perception of any linear system dynamics with only two dimensions: the real and imaginary axes in the complex plane.**

***Index Terms*—Difference threshold, frequency response function (FRF), haptics, just-noticeable difference (JND), mass-spring-damper systems, Weber's law.**

I. Introduction

AT PRESENT, haptic displays are becoming increasingly indispensable in many manual control tasks. By providing the force feedback, a control device (e.g., a manipulator) acts as the haptic interface between a human operator and the system being controlled. More importantly, haptic presentation enables one to physically act upon what one feels, making a task more intuitive [1]–[6].

Depicting the desired system dynamics correctly is important to ensure that operators can rely on their skills to proficiently accomplish tasks. However, the information that the force feedback carries about the system dynamics one intends to present is inevitably distorted. This is due to limitations of control systems and actuators [7], time delays in communication [8], and compromises needed to resolve stability issues [9]–[14].

Aiming for perfect transparency can place excessive, and even unnecessary demands on haptic devices, as *some distortions may not even be perceived* by the human operator. A human-centric assessment is more appropriate to determine whether a particular haptic device performs in a satisfactory way, allowing more room for balance between transparency and stability. To this end, it is crucial to know how large a distortion of the system dynamics must be to provide the human operator with a noticeably different experience of that system. Thresholds for human perception are typically known as *just-noticeable difference* (JND) [15], [16]. Attempts to directly measure the JND in perceiving system dynamics are scarce, however. It is challenging to select representative control variables, and a systematic approach to generalize results from a limited number of studies is currently lacking.

Perception of properties such as inertia or stiffness requires an active manipulation of the device or object being manipulated. In research on "dynamic touch," related work on the perception of higher order properties of manipulated devices has been performed. Examples are—among others—the haptic perception of object length and inertia [17], the perception through nonlinear stiffness of the distance-to-break in biological tissue [18], [19], or the perception of viscosity [20]. This work shows that humans are able to estimate relevant higher order properties from mechanical systems through active manipulation, and that the accuracy with which these properties are estimated follows a Weber–Fechner relationship.

As mass-spring-damper mechanical systems account for the majority of manipulators applied in systems and vehicles where manual control is needed, and in many systems we come across in daily life, many previous studies focus on the JNDs in perceiving changes in stiffness, mass (or inertia), damping or combinations of these [21]–[27]. In general, Weber's law applies when humans sense each of these three properties in isolation. For example, the human JND in spring stiffness, in the case of a system with negligible inertia and damping, is indeed proportional to the selected stiffness [25]. However, the interactions between perceiving any of the three properties are difficult to predict from the isolated measurements. The JND in each property of a mass-spring-damper system seems to be affected by variations in the other two properties. As an example, our ability to discern a change in a system's damping varies with that system's inertia and stiffness properties [28], [29]. This fact, violating Weber's law, limits the generalization of previous findings and the formulation of a general concept. However, as in work on dynamic touch [17], describing the dynamics in an integrated, higher order variable might provide a solution to predicting human accuracy in assessing and matching device dynamics.

Manuscript received November 12, 2019; revised March 2, 2020; accepted April 5, 2020. Date of publication May 25, 2020; date of current version September 15, 2020. This article was recommended by Associate Editor V. Fuccella. *(Corresponding author: Wei Fu.)*

The authors are with the Faculty of Aerospace Engineering, Delft University of Technology, 2629 Delft, HS, The Netherlands (e-mail: W.Fu-1@tudelft.nl; M.M.vanPaassen@tudelft.nl; M.Mulder@tudelft.nl).

Color versions of one or more of the figures in this article are available online at http://ieeexplore.ieee.org.

Digital Object Identifier 10.1109/THMS.2020.2989383

This article explains the current state of the art in modeling human difference thresholds in perceiving system dynamics from force feedback. A part of the results and a preliminary analysis is also published in [30]. In this article, a substantial extension with new evidence that leads to a unified model of human difference threshold is made. We first continue on our latest work [29], explore in depth the characteristics of all JNDs in perceiving mechanical properties, and focus in particular on understanding the interactions between these.

Furthermore, we will bridge the existing gap between JNDs in isolated mechanical properties and the JND in the total dynamics of a system. This connection is based on the fact that a system's behavior perceived by an operator is primarily determined by the *frequency response function* (FRF) of that system. In Section II, we will further elaborate this connection and show that the JND in each of the three mechanical properties in fact represents the FRF's JND in one particular direction in the complex plane. This also allows us to generalize the experimental findings to higher order system dynamics, leading to a unified human threshold model.

The remainder of this article is organized as follows. The following section elaborates on our previous findings, and lays the foundations for the transition from the JNDs in mechanical properties of a mass-spring-damper system to the JNDs in the real- and imaginary-part frequency response of that system. Section III discusses a first experiment, which extends our previously proposed JND rule to systematically describe the interaction between the JNDs in the two complex components. Section IV validates the unified threshold model and shows that the JND in both parts has the same value. Section V generalizes the unified model for the JNDs in the two complex parts, and extends our findings to systems with arbitrary dynamic orders. Section VI discusses the findings, and puts forward challenges for future research. Finally, Section VII summarizes our contributions.

II. Preliminaries

Assume that a haptic control manipulator presents the dynamics of a mass-spring-damper system. Define $H(\omega j)$ as the FRF that describes the relation between the device displacement (or deflection angle) $X(\omega j)$ and the force (or torque) $F(\omega j)$ feedback

$$H(\omega j) = \frac{F(\omega j)}{X(\omega j)} = \underbrace{k - m\cdot\omega^2}_{\Re H(\omega j)} + \underbrace{b\cdot\omega\cdot j}_{\Im H(\omega j)} \tag{1}$$

where $\Re H(\omega j)$ and $\Im H(\omega j)$ denote the real and imaginary components of the complex-valued FRF. These two parts, respectively, determine the in-phase and the out-of-phase force response to the displacement. Note that the imaginary number j means that the force response generated by the system's damping has a 90° phase difference with respect to an input displacement.

The real part $\Re H(\omega j)$ is comprised of the frequency response of system's stiffness k and inertia m, and the imaginary part $\Im H(\omega j)$ is the frequency response of the system's damping b. Thus, changes in a mechanical property can be characterized as changes in one of the two complex parts of system's FRF. One can directly see that changes in the real part could cause the perceived stiffness and inertia to change, and that changes in the imaginary part can lead to variations in the perceived damping.

Hence, the JNDs in the three mechanical properties (m, k, b) can be linked to JNDs in the real and imaginary parts of the system's FRF. This makes it possible to directly study the JND in the dynamics of a system. Our previous studies showed that an interaction exists between human perceptions of stiffness and mass (or inertia), due to the fact that these properties *together* define the real part of the system's frequency responses [29], [31].

It was found that human JNDs in these two mechanical properties are also *coupled*, and can be integrated into the JND in the real-part dynamics [29]

$$\Delta\Re H(\omega j)_{\text{jnd}} = \Delta k_{\text{jnd}} - \Delta m_{\text{jnd}}\cdot\omega^2 \tag{2}$$

where Δk_{jnd} and Δm_{jnd} are the "JND in stiffness" and "the JND in inertia," respectively.

Along similar lines, from (1) one can see that the "damping JND" Δb_{jnd} can be represented by the JND in the imaginary part

$$\Delta\Im H(\omega j)_{\text{jnd}} = \Delta b_{\text{jnd}}\cdot\omega\cdot j. \tag{3}$$

Now, a time-domain variable is a function of time, whereas a frequency-domain variable is a function of *frequency*. Hence, to understand the characteristics of the JNDs in the frequency response [those given by (2) and (3)], we need to collect the measurements at different frequencies.

A convenient approach is to confine haptic interactions to *each individual frequency*. Investigations were carried out at a single frequency of 6 rad/s in our previous study [29]. There, we found that the joint JND in stiffness and mass (or inertia)—the JND in the real part—can be expressed with Weber's law when the system's damping is negligible ($b \approx 0$)

$$\left|\frac{\Delta\Re H(\omega j)_{\text{jnd}}}{\Re H(\omega j)}\right| = \text{constant}. \tag{4}$$

Furthermore, it was found that the human JND in a system's damping is affected by the system's stiffness and inertia. That is, the JND in the imaginary part is affected by the real-part dynamics [29]. Our investigation into this effect demonstrated that this JND is proportional to the magnitude of the system's total frequency response [29]

$$\left|\frac{\Delta\Im H(\omega j)_{\text{jnd}}}{H(\omega j)}\right| = \text{constant}. \tag{5}$$

This equation can be seen as an extension of Weber's law. It also shows the effect of $\Re H(\omega j)$: when the real part $\Re H(\omega j)$ increases, the magnitude of $H(\omega j)$ increases as well, and as a result the JND in the imaginary part (or damping) becomes higher.

Now we have shown that the JND in the imaginary part is affected by the real-part dynamics. An important question that arises, is whether the same holds for the JND in the real part. Based on the fact that these two complex components reflect orthogonal dimensions in the complex plane, one can expect that *both* dimensions will indeed affect each other. It could be

that (4) is in fact a simplification of this universal property, a simplification that excludes the effect of the imaginary component. As can be seen from (1), when a system's damping is negligible, the real component equals the system's frequency response (i.e., $\Re H(\omega j) = H(\omega j)$ when $b = 0$). In this case, (4) and (5) are in fact in the same form. We therefore hypothesize that the effect of the imaginary part on the JND in the real part (i.e., the effect of a system's damping on the JND in that system's stiffness and inertia), can *also* be described by the system's total frequency-response magnitude, in the same way as in (5). The following two sections present two experiments performed to investigate this hypothesis, and others, to obtain a unified model for *all* human thresholds in perceiving dynamics with haptic force feedback manipulators.

III. Experiment 1: Revisiting the JND in Perceiving Real-Part Dynamics

A. Method

1) Dependent and Independent Variables: To test our hypothesis, the first experiment will study the effect of $\Im H(\omega j)$ on $\Delta\Re H(\omega j)_{\mathrm{jnd}}$, and in particular, to examine whether this effect can also be expressed using the model given in (5). To this end, mass-spring-damper systems that differ in the imaginary-part dynamics will be used to measure $\Delta\Re H(\omega j)_{\mathrm{jnd}}$. To extend the model, investigations will be conducted at different manipulator movement frequencies ω.

In addition, the model needs to be validated under different *signs* of the real-part dynamics. As can be seen from (1), the sign of $\Re H(\omega j)$ depends on the stiffness and inertia properties, as well as on the current input frequency. This FRF component acts as a gain, and the force response it generates can be expressed as

$$F_{si}(\omega j) = X(\omega j) \cdot |\Re H(\omega j)| \cdot e^{j\angle \Re H(\omega j)}$$
$$\text{where } \angle \Re H(\omega j) = \begin{cases} 0^\circ & \text{if } \Re H(\omega j) > 0 \\ 180^\circ & \text{if } \Re H(\omega j) < 0 \end{cases}. \tag{6}$$

Hence, a spring force that resists the manipulator displacement is produced when $\Re H(\omega j) > 0$; an inertia force proportional to the acceleration is produced when $\Re H(\omega j) < 0$. These two force responses have opposite directions. To ensure that the model can describe the JND in the real part of a system's FRF over the entire complex plane, evaluation of different response directions must be conducted.

2) Experimental Conditions: The experiment has nine conditions. Table I lists the exact system parameters and independent variables, and Fig. 1 shows the system dynamics defined by the nine conditions in the complex plane. Note that the numbers are given with a rotational unit (e.g., N·m for force and rad for displacement). As can be seen, the JND for each condition will be measured at a single frequency of haptic interaction ω_i. This will be achieved by asking our subjects to track a sinusoidal signal during the experiment, such that they will be able to apply (an approximately) sinusoidal movement to the manipulator. Section III-A6 describes the tracking task in greater detail.

Conditions C1–C5 measure the JND in a positive $\Re H(\omega_i)$, which contributes a spring behavior, at an input frequency of 6 rad/s. In addition, they define five levels of $\Im H(\omega_i)$, the ratio of which to $\Re H(\omega_i)$, r, ranges from 0 to 2. Measurements for these five conditions will show how $\Im H(\omega_i)$ affects $\Delta\Re H(\omega_i j)_{\mathrm{jnd}}$. To test the effect of the input frequency, conditions C6 and C7 define a movement frequency of 8 rad/s. The effect will be evaluated at two different ratios between the two complex parts. Conditions C8 and C9 define a negative $\Re H(\omega_i)$, which generates an inertia response, to study the effect of the system's response direction (the sign of $\Re H(\omega_i j)$) on the JND. These two conditions differ in the ratio between the two complex components.

TABLE I
Conditions of Experiment 1

Condition	$\Re H(\omega_i j)$	$\Im H(\omega_i j)$	ω_i [rad/s]	$r=\left\lvert\frac{\Im H(\omega_i j)}{\Re H(\omega_i j)}\right\rvert$
C1	1.26	0.00	6	0.0
C2	1.26	0.63	6	0.5
C3	1.26	1.26	6	1.0
C4	1.26	1.89	6	1.5
C5	1.26	2.52	6	2.0
C6	1.26	0.00	8	0.0
C7	1.26	2.52	8	2.0
C8	−1.26	0.00	6	0.0
C9	−1.26	2.52	6	2.0

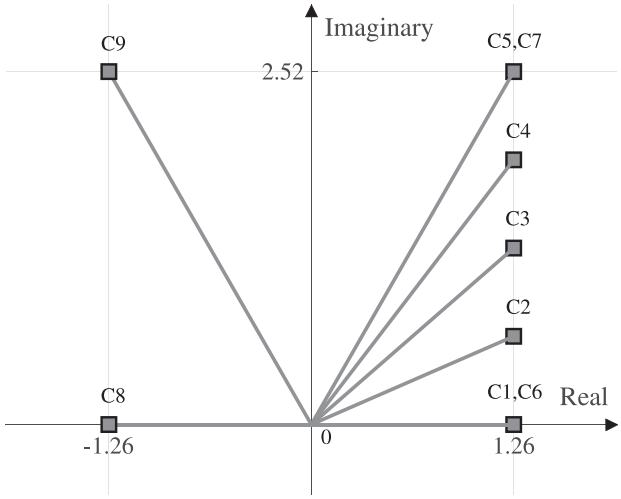

Fig. 1. Experimental conditions shown on the complex plane.

The system dynamics defined in Table I are realized using mass-spring-damper systems. The three parameters k, m, and b [see (1)] are set according to the following rule to obtain the desired values of $\Re H(\omega_i)$ and $\Im H(\omega_i)$:

$$k = \begin{cases} \Re H(\omega_i j) + 0.01{\omega_i}^2 & \text{if } \Re H(\omega_i j) > 0 \\ 0 & \text{if } \Re H(\omega_i j) < 0 \end{cases}$$
$$m = \begin{cases} 0.01 & \text{if } \Re H(\omega_i j) > 0 \\ \dfrac{-\Re H(\omega_i j)}{\omega_i^2} & \text{if } \Re H(\omega_i j) < 0 \end{cases} \tag{7}$$
$$b = \frac{\Im H(\omega_i j)}{\omega_i j}.$$

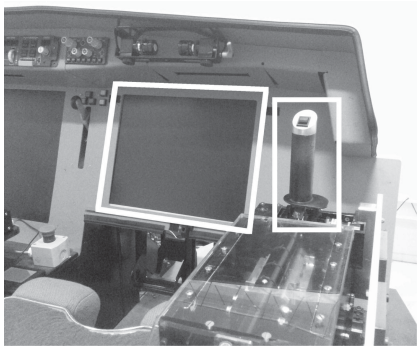

(a)

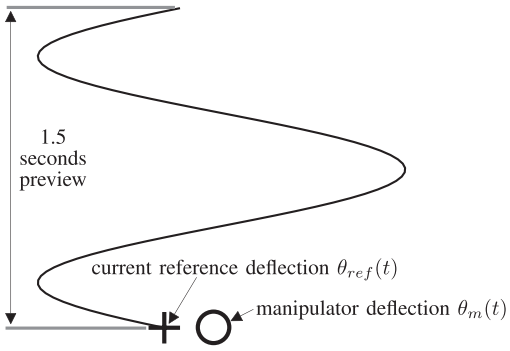

(b)

Fig. 2. (a) Experimental devices (i.e., the side-stick manipulator and the LCD screen). (b) Details of the tracking task that was shown on the LCD screen.

In this article, units of these three parameters are: N·m/rad for k, N·ms/rad for b, and kg·m^2 for m.

As shown by (1), at each single frequency the combination of k and m that leads to a particular $\Re H(\omega_i j)$ is not unique. In other words, the condition settings defined in Table I can in fact be realized by an infinite number of systems with different stiffness and inertia (these systems have the exact same harmonic response to the sinusoidal input defined at the corresponding frequency). In order to measure human JND in the system dynamics using the staircase procedure given in Section III-A5, a criterion should be available for subjects. By using the parameter settings obtained via (7), measuring $\Delta\Re H(\omega_i j)_{\mathrm{jnd}}$ can be simplified into measuring the stiffness JND (for conditions where $\Re H(\omega j) > 0$) and the inertia JND (for conditions where $\Re H(\omega_i j) < 0$). Ideally, the inertia m in (7) should be set to zero for $\Re H(\omega_i j) > 0$. However, a minimal setting for the inertia of $0.01\ \mathrm{kgm}^2$ has to be maintained to guarantee the system stability.

3) Experimental Devices: The experiment was conducted in TU Delft's Human–Machine Interaction Laboratory, with Fig. 2(a) illustrating the used devices. A side-stick manipulator (an admittance haptic device) driven by an electro-hydraulic actuator was used to present the mass-spring-damper systems defined by the experimental conditions. Position of the manipulator and the moment that the subject exerts on the manipulator are led through low-pass filters (bandwidth = 200 Hz) before being read into the laboratory computer at the execution frequency of the manipulator's control system (2500 Hz). The position-following bandwidth of the manipulator's control system is around 40 Hz. Therefore, the desired system dynamics at the desired input frequencies (around 1 Hz) can be accurately realized. The manipulator is equipped with a handle with a diameter of 35 mm, which provides grooves for placement of the fingers. When the subject correctly places his/her hand on the handle, the center of the hand is 90 mm above the manipulator rotation axis. The manipulator can be deflected in the left/right direction (lateral) like a joystick, and its motion in fore/aft direction is fixed at the neutral position. During the experiment, an liquid-crystal display (LCD) screen was placed in front of the subject to assist the subject in realizing the prescribed sinusoidal manipulator movement (see Section III-A6 for information about the tracking task).

4) Participants: The experiment was performed by nine subjects, who were all right-handed and did not have a history of impairments in moving their arms or hands. The experiment was approved by the Human Research Ethics Committee of TU Delft, and informed consent was obtained. Sufficient training was performed by all subjects before the measurements started.

5) Experimental Procedure: This study only investigates the upper JNDs (the threshold for perceiving an increase in the stimulus). A one-up/two-down staircase approach [32] was adopted to measure the JND. In general, the staircase procedure needed approximately 20–30 runs to finish. Each run consisted of two 6.3-s simulations. In one of the two simulations, the manipulator realized the reference system dynamics defined by the experimental condition being tested [see Table I and (7)]. In the other simulation, the subject experienced a controlled system, which only differed from the reference system in the mechanical property being tested (stiffness in the case of conditions C1–C7 where $\Re H(\omega_i j) > 0$, inertia in the case of conditions C8–C9 where $\Re H(\omega_i j) < 0$). The sequence of the two simulations in each run was randomly based on a prior probability of 0.5.

The difference in the corresponding mechanical property between the two systems was an adjusted increment. Therefore, the controlled system had higher stiffness or inertia than the reference system. In each simulation, the subject needed to interpret the manipulator dynamics while moving the manipulator with the prescribed sinusoidal movement. After each experimental run, the subject was required to answer in which of the two simulations (s), he experienced the stronger manipulator stiffness (in the case of conditions C1–C7) or the higher manipulator inertia (in the case of conditions C8–C9). The increment for the next run was then adjusted according to the correctness of the subject's answer, and would gradually converge to the upper JND. Readers are referred to our previous work [29] for more details about this staircase procedure.

6) Tracking Task: Our subjects were asked to perform a preview tracking task [33] in each simulation to ensure that they would interact with the side-stick manipulator at the desired frequencies. Fig. 2(b) shows the details of the task. The reference manipulator deflection angle is a sine signal

$$\theta_{\mathrm{ref}}(t) = 0.37 \cdot \sin(\omega_i t). \tag{8}$$

TABLE II
JND MEASUREMENTS (MEAN ± 95%CI)

Conditions	$\Delta\Re H_{jnd}(\omega_i j)$ (how it is obtained)	ratio $r=\left\lvert\frac{\Im H(\omega_i j)}{\Re H(\omega_i j)}\right\rvert$				
		0.0	0.5	1.0	1.5	2.0
C1-5	$\Delta\Re H_{jnd}(\omega_i j)$ $(=\Delta k_{jnd})$	$.15 \pm .07$	$.15 \pm .05$	$.22 \pm .05$	$.27 \pm .06$	$.34 \pm .05$
C6-7	$\Delta\Re H_{jnd}(\omega_i j)$ $(=\Delta k_{jnd})$	$.14 \pm .04$	-	-	-	$.29 \pm .06$
C8-9	$\Delta\Re H_{jnd}(\omega_i j)$ $(=\Delta m_{jnd}\cdot\omega_i^2)$	$.16 \pm .05$	-	-	-	$.30 \pm .08$

Here, the deflection angle is given in radians. ω_i is the desired frequency of the manipulator movement (6 or 8 rad/s, see Table I). In the experiment, the first and last full cycle of the sine signal were used as fade-in and fade-out phases. During the fade-in phase, the amplitude of the reference signal linearly increases from 0 to 0.37. During the fade-out phase, it decreases from 0.37 to 0.

The subject was encouraged to reduce the tracking error as possible as (s)he could. The tracking error is the difference between the current manipulator deflection $\theta_m(t)$ [the "$\circ$" in Fig. 2(b)] and the current reference deflection $\theta_{\mathrm{ref}}(t)$ (the "+"). These two symbols can only move horizontally, corresponding to the lateral movement of the manipulator. The visual preview of the reference is shown as a winding curve. It presents 1.5-s future information about the reference signal θ_{ref}.

B. Results

All participants performed the tracking task well. We evaluated the actual manipulator movement frequencies in all the experimental runs. The average frequency only deviates from the desired values by less than 2%. This ensures that the experimental observations accurately reflect the effects of the independent variables under the desired conditions.

Table II and Fig. 3 show the JND measurements, expressed with subjects' means and 95% confidence intervals corrected for between-subject variability. When examining the JNDs measured under conditions C1–C5 (systems with the same stiffness and inertia, but different damping), it can be seen that the JND exhibits a clear increase as the ratio between the two complex components (r) increases. The result from a one-way repeated measures analysis of variance (ANOVA) indeed reveals a significant effect of r ($F(4, 32) = 8.1, p < 0.01$).

Two one-way repeated measures ANOVAs are carried out independently to examine: 1) the differences among conditions C1, C6, and C8; and 2) the differences among conditions C5, C7, and C9. Results show that when the damping of the system presented to our subjects is negligible (i.e., $r = 0.0$, conditions C1, C6, and C8), the changes in the input movement frequency (ω_i) and the response direction (the sign of $\Re H(\omega_i)$) do not have any significant effect on the JNDs ($F(2, 16) = 0.21, p > 0.05$). When the damping of the presented system is high (i.e., $r = 2.0$, conditions C5, C7, and C9), the same conclusion can be drawn ($F(2, 16) = 0.74, p > 0.05$).

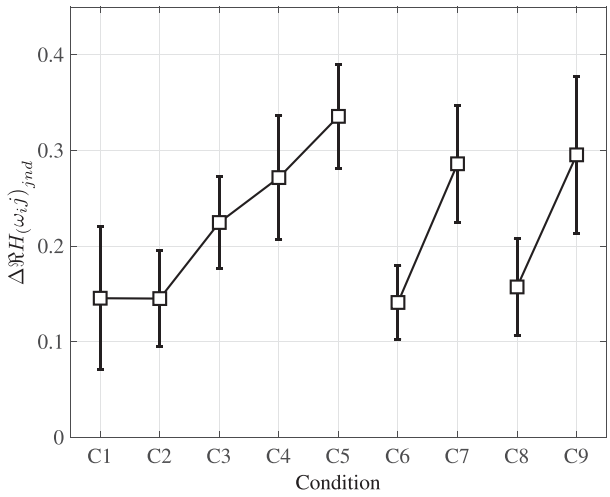

Fig. 3. Measured $\left\lvert\Delta\Re H(\omega_i j)_{\mathrm{jnd}}\right\rvert$, which is shown with the subjects' means and 95% confidence intervals corrected for between-subject variability.

These results confirm our hypothesis that the imaginary part of the system's dynamics affects the resolution of human perception of the system's response generated by the real part (i.e., $\Im H(\omega j)$ affects $\Delta\Re H(\omega j)_{\mathrm{jnd}}$). The JND in a system's stiffness and inertia violates Weber's law when the system's damping varies (since Weber's law expects no differences among conditions C1–C5, between conditions C6 and C7, or between conditions C8 and C9). In addition, the JND in the real-part dynamics and the effect of the imaginary part on it are *independent* of changes in the sign of the real part and variations in the input movement frequency. In other words, humans have *similar* thresholds for perceiving changes in the spring and inertia forces, and these thresholds remain approximately constant over a relatively low-frequency range. When a system possesses higher damping, inertia and stiffness changes must be larger before humans are able to notice these differences.

C. Model Validation

To examine whether the JND in the real part can also be described by the model given in (5), the measured JND for each condition is normalized to the magnitude of the frequency

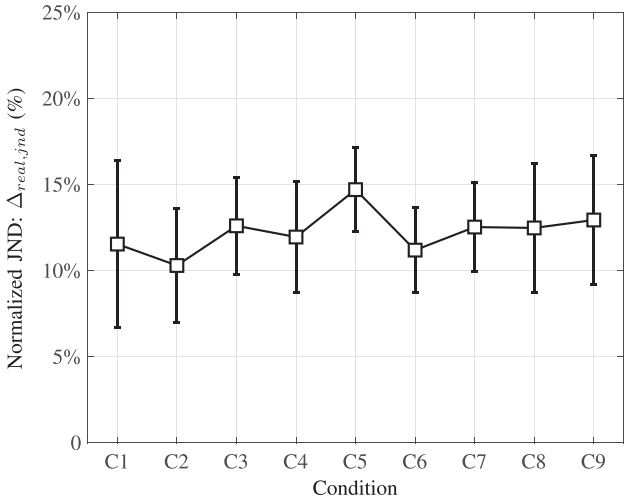

Fig. 4. Ratio of the measured $\left|\Delta\Re H(\omega_i)_{\mathrm{jnd}}\right|$ to $|H(\omega_i j)|$ (i.e., the normalized JNDs). The ratios for different conditions are shown with the sample means and 95% confidence intervals corrected for between-subject variability.

response of the corresponding system, according to

$$\Delta_{\mathrm{real,jnd}} = \left|\frac{\Delta\Re H(\omega_i j)_{\mathrm{jnd}}}{H(\omega_i j)}\right|. \tag{9}$$

Fig. 4 shows $\Delta_{\mathrm{real,jnd}}$ for all conditions. The normalized JNDs remain approximately constant over the nine conditions, with an average of 12.2%. The result from a one-way repeated-measures ANOVA shows that there is no significant difference among the conditions ($F(8, 64) = 0.59, p > 0.05$). The validity of the model is therefore confirmed, indicating that the magnitude of $\Delta\Re H(\omega j)_{\mathrm{jnd}}$ is proportional to the magnitude of $H(\omega j)$.

This finding leads to an extension of Weber's law for the joint JND in stiffness and inertia. When considering the frequency response of the system to be the reference stimulus, the relative change in its real-part dynamics, which alters the perception, is constant

$$\left|\frac{\Delta\Re H(\omega j)_{\mathrm{jnd}}}{H(\omega j)}\right| = \left|\frac{\Delta k_{\mathrm{jnd}} - \Delta m_{\mathrm{jnd}} \cdot \omega^2}{k - m \cdot \omega^2 + b \cdot \omega \cdot j}\right| = \text{constant}. \tag{10}$$

D. Discussion

Experiment 1 demonstrates the effect of a system's damping on human perception of the system's stiffness and inertia. The observed variations in the JNDs caused by the changes in the damping cannot be properly described by Weber's law. As expected, the joint JND in stiffness and inertia increases as the system's damping increases.

The results provide some useful insights into the transparency evaluation of haptic interfaces, in terms of the displayed stiffness and inertia. On the one hand, higher system damping allows for larger distortions of stiffness and inertia. The high demands put on the control system and hardware, when simulating small inertia and high stiffness, can therefore be alleviated. This will in turn allow for a greater stability margin. On the other hand, an increase in a system's damping can reduce the human ability to discern changes in the system's stiffness and inertia properties. This effect must be considered by designers when additional damping is added into the system dynamics, e.g., in order to improve the stability of the system [14], [34].

Our previous work [29], [31] allows us to relate human perception of the three mechanical properties of a mass-spring-damper system to the real and imaginary parts of the system's dynamics. The current study reveals an effect of the imaginary part on the JND in the real part. This effect is similar to that shown by our previous study between the real part and the JND in the imaginary part [29]. Results show that these mutual interactions can be described by a unified rule, which suggests that the JND in each complex part is proportional to the total system's frequency-response magnitude $|H(\omega j)|$.

The results also show that the model is able to describe the JND for different movement frequencies. Although the experiment investigates only a relatively small variation in the frequency, our findings can still be applied to a wide range of manual control tasks, where the input movement is predominantly produced by the human arm (such as car driving and aircraft flying). This is because in these tasks the frequency content of human control inputs mainly appears at a low-frequency range (usually below 2 Hz), which is limited by the neuromuscular system [35].

IV. Experiment 2: Generalizing the JND in System Dynamics

Experiment 1 showed that the JNDs in the real and imaginary parts are governed by the same rule [see (5) and (10)]. In this section, we discuss the results of a second experiment, which was set up to investigate whether or not the two JNDs can be described by the same ratio, that is, whether the *same constant* applies to both (5) and (10).

A. Method

1) Dependent and Independent Variables: The experiment draws comparisons between the JND in the real-part dynamics and the JND in the imaginary-part dynamics. Three input frequencies ω were tested. At each frequency, the two JNDs were obtained from only one system. This is because the JND rules (i.e., the proportional relation) stated by (5) and (10) are independent of the system dynamics (i.e., no matter how the denominator changes, the proportional relation will not change). Thus, the finding obtained from a single system is representative and applies to all other systems.

A factorial design results in six conditions, listed in Table III. For simplicity, the real and imaginary parts of the system dynamics tested in the experiment are the same (i.e., $\Re H(\omega_i j) = \Im H(\omega_i j)$). In addition, the magnitude of these two parts is kept the same for all the three frequencies. One can imagine that $H(\omega_i j)$ is always the same vector in the complex plane, with equal projections on the two axes.

2) Procedure: The desired system dynamics were realized using mass-spring-damper systems. (7) was used to obtain the corresponding stiffness, inertia, and damping coefficients [k, m, and b in (1)]. These parameters were simulated using the same side-stick manipulator that is described in Section III-A3. The

TABLE III
CONDITIONS OF EXPERIMENT 2

Condition	Measured JND	$\Re H(\omega_i j)$	$\Im H(\omega_i j)$	ω_i [rad/s]
C1	$\Delta\Re H(\omega_i j)_{jnd}$	1.50	1.50	5.0
C2	$\Delta\Im H(\omega_i j)_{jnd}$	1.50	1.50	5.0
C3	$\Delta\Re H(\omega_i j)_{jnd}$	1.50	1.50	6.5
C4	$\Delta\Im H(\omega_i j)_{jnd}$	1.50	1.50	6.5
C5	$\Delta\Re H(\omega_i j)_{jnd}$	1.50	1.50	8.0
C6	$\Delta\Im H(\omega_i j)_{jnd}$	1.50	1.50	8.0

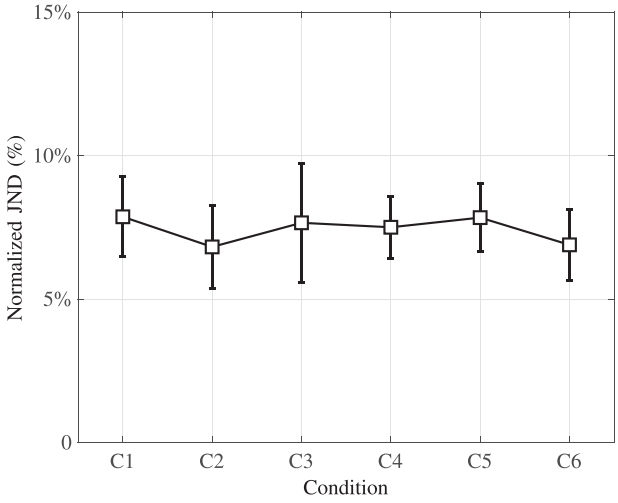

Fig. 5. Normalized JNDs in the real and imaginary parts, shown with the subjects' means and 95% confidence intervals corrected for between-subject variability.

JNDs were measured by the same adaptive staircase procedure described in Section III-A5. When measuring the JND in the real part (conditions C1, C3, and C5), the subject was asked to identify the simulation with the stronger manipulator stiffness. When measuring the JND in the imaginary part (conditions C2, C4, and C6), the subject was asked to identify the simulation with the higher manipulator damping. The same tracking task described in III-A6 was performed by subjects to ensure that the haptic interaction would occur at the desired frequencies.

3) Participants: Six subjects participated. They all are right-handed and did not have any history of impairments in moving their arms or hands. This experiment was approved by the Human Research Ethics Committee of TU Delft. Informed consent was obtained from all participants. All subjects received sufficient training before the formal experiment.

B. Results

All participants performed the tracking task well. The averages of the actual movement frequencies over all experimental runs only deviate from the corresponding desired frequencies by less than 2%. This indicates that the intended effects of the independent variables are indeed accurately reflected by the results.

Fig. 5 shows the JND measurements. Here, the JNDs in the two complex parts are normalized to the frequency-response magnitude of the corresponding systems [similar as in Fig. 4, see (9)]. As can be seen from the figure, the JNDs under the six conditions are approximately the same, with an average of 7.5%. A one-way repeated measures ANOVA showed no significant difference among conditions ($F(5, 25) = .57, p > .05$). Therefore, the JNDs in both parts of a system's dynamics can be expressed with our extended Weber's law *using the same constant*, which is (for the frequencies analyzed) *independent of the movement frequency*

$$\left|\frac{\Delta\Re H(\omega j)_{\text{jnd}}}{H(\omega j)}\right| \approx \left|\frac{\Delta\Im H(\omega j)_{\text{jnd}}}{H(\omega j)}\right| = \text{constant}. \tag{11}$$

This finding allows us to describe the JNDs in stiffness, inertia, and damping with one, *unified* model, which clearly shows how the JNDs in three mechanical properties of a mass-spring-damper system can be related to the JND in perceiving changes in system dynamics.

V. UNIFIED JND MODEL FOR SYSTEM DYNAMICS

A. Unified Difference Threshold in Perceiving System Dynamics

In fact, any change in the system dynamics can always be represented by changes in the real and imaginary parts of the FRF. For example, define a change in the FRF of a mass-spring-damper system as $\Delta H(\omega j)$, which is caused by changes in the three mechanical properties. The complex-valued $\Delta H(\omega j)$ can be expressed by its two components

$$\Delta H(\omega j) = \underbrace{\Delta k - \Delta m \cdot \omega^2}_{\Delta\Re H(\omega j)} + \underbrace{\Delta b \cdot \omega \cdot j}_{\Delta\Im H(\omega j)} \tag{12}$$

where Δk, Δm, and Δb denote changes in stiffness, inertia, and damping, respectively.

This means that $\Delta H(\omega j)$, independent of the parameters that cause it, will alter the human perception of the system once the threshold for perceiving changes in either of the two components is exceeded. In other words, JNDs in these two parts, as defined by (11), in fact represent the JND in $H(\omega j)$.

At the movement frequencies where the haptic interaction takes place, any dynamics change that exceeds such a JND will lead humans to perceive the system differently. At each individual frequency, (11) defines the intervals for imperceptible changes in the system's projections on the two axes of the complex plane.

For a straightforward illustration, Fig. 6 gives an example that shows the dynamics of an arbitrary system at a single frequency. In the complex plane, the system's FRF—$H(\omega j)$—at a single frequency is represented by a vector (the black line). The real- and imaginary-part dynamics determine the projections on the two axes, respectively. A change in the system dynamics will result in a different vector, which has at least one different projection, as shown by the red and blue vectors. The JNDs in the two complex parts become intervals on the two axes. Therefore, changes in each projection within the corresponding interval cannot be perceived by humans. These two intervals

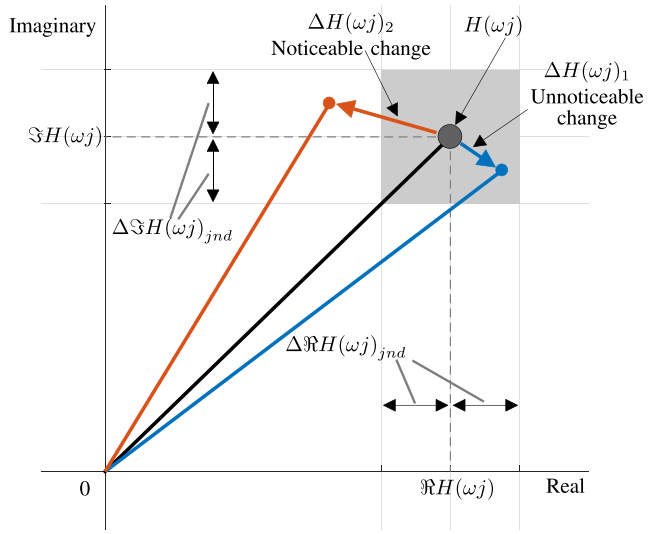

Fig. 6. Illustration of the threshold for altered perception of the system dynamics. The base dynamics are depicted by the dark gray circle. The JND thresholds are indicated on the axes and by the shaded square. The JNDs are proportional to the system's frequency-response magnitude, which is the length of the black vector. Dynamics changes within the threshold are not perceptible (e.g., the blue vector), whereas those exceeding the threshold alter the perception of the system (e.g., the red vector).

form a threshold region (the shaded square), and any change in dynamics that lies within this region does *not alter* how humans perceive that system. A change in system dynamics will only lead humans to have a different perception when that change exceeds the threshold region.

Fig. 7 illustrates the difference thresholds corresponding to a system, at multiple frequencies. We show a second-order system with typical stiffness, inertia, and damping properties (i.e, $k = 2.5\,\text{N·m/rad}, m = 0.022\,\text{kgm}^2, b = 0.3\,\text{N·ms/rad}$). The dynamics of the system, $H(\omega j)$, are shown as the black curve; the arrow of the curve indicates an increase in the input frequency ω. As can bee seen, the thresholds at different frequencies (represented by gray squares) are different in size. As the JNDs in the two complex components are proportional to the magnitude of the system's frequency response [see (11)], the threshold region becomes larger as the system's magnitude increases. For example, to alter what humans feel about the system, a larger change in the system's dynamics will be needed at the movement frequency of 14 rad/s than at the frequency of 6 rad/s.

Furthermore, the threshold model proposed in this study is not limited to only mass-spring-damper systems, systems that have second-order dynamics. Although the system dynamics (i.e., Tables I and III) are realized using second-order systems in the experiments, the results would not change if higher order systems were used. In fact, two systems with different orders can have exactly the same FRF at a particular frequency (i.e., the frequency where the two FRFs cross). One can imagine that the dynamics of a higher order system at a single frequency can always be matched by a second-order system. At this frequency, the two systems will be perceived to be the same [31] and there is no reason why the JND threshold would not be identical. Therefore, the model given in (11) is *independent* of the system dynamics order, representing human perceptual resolution of all systems.

This frequency-domain model can be used to evaluate the transparency of haptic interfaces via examining the differences between the desired dynamics and the presented dynamics at the frequencies of interest (or over the frequency range where the haptic interaction is expected to occur). A haptic device can potentially cause a noticeable distortion if there exists a frequency at which the difference exceeds the corresponding threshold. This allows for understanding *whether and when* an operator's haptic experience is affected by limiting factors behind a particular application, such as the bandwidth of the control system, inherent actuator dynamics, transmission time delays, and the performance sacrifice made for stability issues.

VI. Discussion

Through a second experiment, we find that the JNDs in perceiving the two complex components of system dynamics are approximately the same, and are both proportional to the system's frequency-response magnitude. The findings also apply to systems with arbitrary orders. This allows us to further extend Weber's law for the JND in system dynamics. When considering the frequency response $H(\omega j)$ to be the stimulus, the JNDs in its real and imaginary parts are proportional to its magnitude, $|H(\omega j)|$.

However, possibly due to differences between subjects and the fact that the experiments were carried out at a different time, the measured Weber fractions—the values of the constants in (10) and (11), as well as those collected in our previous work [29]—differ slightly. A larger number of subjects will be necessary to obtain a more representative result.

In the experiments, the JNDs in the two complex components were measured independently. As changes in a system's dynamics along each axis can be reflected in changes in the perception of a particular mechanical property, the independent investigation allowed subjects an intuitive criterion for discerning the dynamic difference presented to them (i.e., identifying the system with the greater stiffness, inertia, or damping). As a result, two independent thresholds were obtained, one corresponding to the real-part changes and the other corresponding to the imaginary-part changes.

However, the interaction between the two thresholds cannot be predicted from the present experiment. It is possible that the *noticeable* change in one part may be affected by an *unnoticeable* change in the other part. Moreover, advances in understanding human haptic perception, particularly those in dynamic (effortful) touch, have shown evidence of direct human perception of higher order invariants [36], [37], such as the inertia tensor (the rotational inertia) in heaviness perception [38], and the "distance-to-brake" in identifying the break points of compliant materials [19]. Therefore, we hypothesize that the JND rule can be further extended into a formula based on a lumped difference in system dynamics

$$\left| \frac{\Delta H(\omega j)_{\text{jnd}}}{H(\omega j)} \right| = \text{constant}. \tag{13}$$

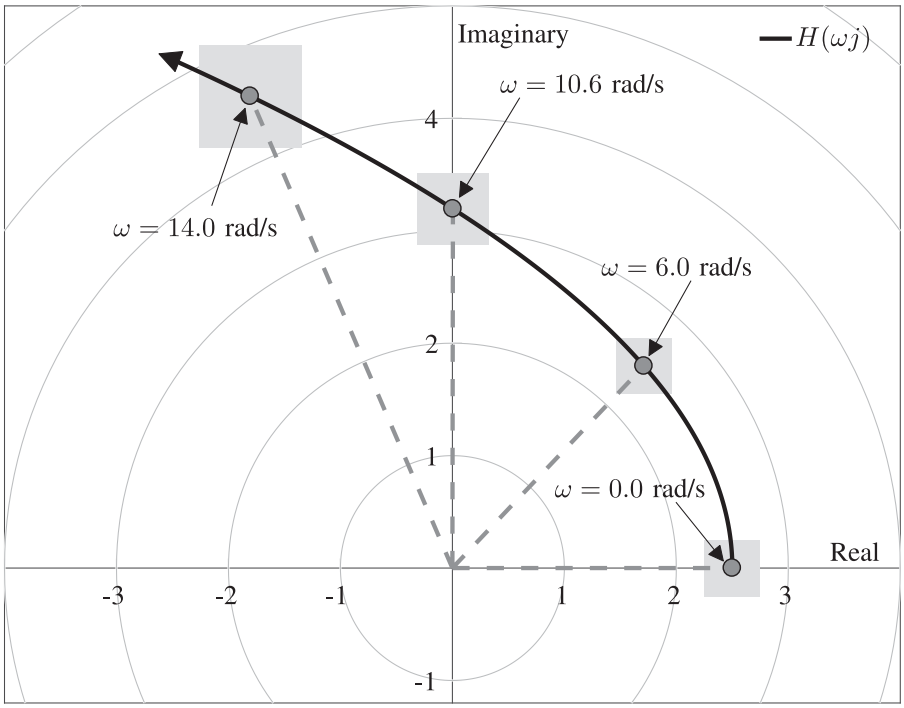

Fig. 7. Example of the threshold for changes in human perception of a typical mass-spring-damper system. The FRF of the system is shown as the black curve, with its arrow indicating the increase in the frequency of excitation. The threshold regions at four different frequencies are given to illustrate the correlation between the threshold size and the magnitude of the system's frequency response.

Equation (13) describes the change in the frequency response of a system as a whole, rather than going into the detailed changes in the two complex parts. The system dynamics at the tested frequency $H(\omega j)$ (or its magnitude $|H(\omega j)|$) can be postulated as the higher order construct perceived by humans, and the JND for this construct is in line with Weber's law, describing a relation between a reference stimulus and a direct change in it that causes a different perception. We have, for lack of evidence from the experiments so far, depicted the threshold region as a square (see Fig. 6); however, it might be possible that it is circular, or elliptic, with a radius proportional to the length of the vector (i.e., the magnitude of the system's frequency response at this frequency).

However, confirming this hypothesis is nontrivial. Measuring the thresholds for changes in different directions in the complex plane (e.g., by introducing changes into both real and imaginary components) would be needed for this. It requires a methodology different from the one used in this article. The current methodology required subjects to identify the change in a single mechanical property (i.e., identify the heavier/stiffer or better-damped system). This is not appropriate for a system dynamics change in an *arbitrary* direction, which may be associated with changes in the perception of more than one property. When determining the JND in noncardinal directions, i.e., combined changes in inertia or stiffness, respectively, damping, there will not always be a meaningful way in which participants can name the differences, e.g., in terms of heavier/stiffer/more or less damping. Devising a new method is therefore necessary for future relevant research.

As already discussed in Section III-D, our findings are currently limited to a relatively low-frequency range. In addition, this study is restricted to *linear* systems and *continuous* haptic interaction. The model has not yet been verified for systems that have a considerable nonlinearity (such as strong friction), and does not account for the effects of transient responses that may occur when sudden changes in system dynamics occur, e.g., the changes upon contact with a stiff wall. Despite these limitations, the proposed JND model already covers a wide range of applications, such as [39]–[41]. Extensions of the model to include nonlinearities and transient responses are topics for future work.

VII. Conclusion

Extending previous work on just-notable-differences in haptic perception, the results of two experiments are described. We conclude that, first, the human perception of the real and imaginary parts of the system dynamics frequency response is governed by the same rule. Our unified model states that JNDs in the two components of the FRF are both proportional to the magnitude of the system frequency response. Second, results show that these two JNDs have the same ratio. Third, the proposed unified JND model applies to systems with arbitrary orders of dynamics. The main result is an extension of Weber's law, and states that a single ratio describes the thresholds for perceiving changes in the two dimensions (real, imaginary) of the complex-valued FRF defining haptic force feedback of system dynamics.

REFERENCES

[1] J. Rebelo, T. Sednaoui, E. B. den Exter, T. Krueger, and A. Schiele, "Bilateral robot teleoperation: A wearable arm exoskeleton featuring an intuitive user interface," *IEEE Robot. Autom. Mag.*, vol. 21, no. 4, pp. 62–69, Dec. 2014.

[2] J. G. W. Wildenbeest, D. A. Abbink, and J. F. Schorsch, "Haptic transparency increases the generalizability of motor learning during telemanipulation," in *Proc. World Haptics Conf.*, Daejeon, South Korea, Apr. 2013, pp. 707–712.

[3] A. M. Okamura, "Haptic feedback in robot-assisted minimally invasive surgery," *Current Opinion Urol.*, vol. 19, no. 1, pp. 102–107, 2009.

[4] R. J. Stone, "Haptic feedback: A brief history from telepresence to virtual reality," in *Proc. Int. Workshop Haptic Human–Comput. Interact.*, Glasgow, U.K., Aug. 2001, pp. 1–16.

[5] X. Hou, R. Mahony, and F. Schill, "Comparative study of haptic interfaces for bilateral teleoperation of VTOL aerial robots," *IEEE Trans. Syst., Man, Cybern., Syst.*, vol. 46, no. 10, pp. 1352–1363, Oct. 2016.

[6] P. F. Hokayem and M. W. Spong, "Bilateral teleoperation: An historical survey," *Automatica*, vol. 42, no. 12, pp. 2035–2057, 2006.

[7] N. Colonnese and A. M. Okamura, "M-width: Stability, noise characterization, and accuracy of rendering virtual mass," *Int. J. Robot. Res.*, vol. 34, no. 6, pp. 781–798, 2015.

[8] S. Hirche and M. Buss, "Human perceived transparency with time delay," in *Advances in Telerobotics*, M. Ferre, M. Buss, R. Aracil, C. Melchiorri, and C. Balaguer, Eds. Berlin, Germany: Springer, 2007, pp. 191–209.

[9] B. Hannaford, "Stability and performance tradeoffs in bi-lateral telemanipulation," in *Proc. Int. Conf. Robot. Autom.*, Scottsdale, AZ, USA, May 1989, vol. 3, pp. 1764–1767.

[10] D. A. Lawrence, "Stability and transparency in bilateral teleoperation," *IEEE Trans. Robot. Autom.*, vol. 9, no. 5, pp. 624–637, Oct. 1993.

[11] R. J. Adams and B. Hannaford, "Stable haptic interaction with virtual environments," *IEEE Trans. Robot. Autom.*, vol. 15, no. 3, pp. 465–474, Jun. 1999.

[12] R. Daniel and P. McAree, "Fundamental limits of performance for force reflecting teleoperation," *Int. J. Robot. Res.*, vol. 17, no. 8, pp. 811–830, 1998.

[13] G. Niemeyer and J. J. E. Slotine, "Stable adaptive teleoperation," *IEEE J. Ocean. Eng.*, vol. 16, no. 1, pp. 152–162, Jan. 1991.

[14] B. Hannaford and J. H. Ryu, "Time-domain passivity control of haptic interfaces," *IEEE Trans. Robot. Autom.*, vol. 18, no. 1, pp. 1–10, Feb. 2002.

[15] S. Feyzabadi, S. Straube, M. Folgheraiter, E. A. Kirchner, S. K. Kim, and J. C. Albiez, "Human force discrimination during active arm motion for force feedback design," *IEEE Trans. Haptics*, vol. 6, no. 3, pp. 309–319, Jul–Sep. 2013.

[16] X. D. Pang, H. Z. Tan, and N. I. Durlach, "Manual discrimination of force using active finger motion," *Perception Psychophys.*, vol. 49, no. 6, pp. 531–540, 1991.

[17] M. T. Turvey, "Dynamic touch," *Amer. Psychologist*, vol. 51, no. 11, pp. 1134–1152, 1996.

[18] L. S. Hartman, I. Kil, C. C. Pagano, and T. Burg, "Investigating haptic distance-to-break using linear and nonlinear materials in a simulated minimally invasive surgery task," *Ergonomics*, vol. 59, no. 9, pp. 1171–1181, 2016.

[19] B. M. Altenhoff, C. C. Pagano, I. Kil, and T. C. Burg, "Learning to perceive haptic distance-to-break in the presence of friction," *J. Exp. Psychol., Human Perception Perform.*, vol. 43, no. 2, pp. 231–244, 2017.

[20] W. M. Bergmann Tiest, A. C. L. Vrijling, and A. M. L. Kappers, "Haptic perception of viscosity," in *Haptics: Generating and Perceiving Tangible Sensations*, vol. 6191, A. M. L. Kappers, J. B. F. van Erp, W. M. Bergmann Tiest, and F. C. T. van der Helm, Eds. Berlin, Germany: Springer, 2010, pp. 29–34.

[21] L. A. Jones and I. W. Hunter, "A perceptual analysis of stiffness," *Exp. Brain Res.*, vol. 79, no. 1, pp. 150–156, 1990.

[22] L. A. Jones and I. W. Hunter, "A perceptual analysis of viscosity," *Exp. Brain Res.*, vol. 94, no. 2, pp. 343–351, 1993.

[23] H. Z. Tan, N. I. Durlach, G. L. Beauregard, and M. A. Srinivasan,, "Manual discrimination of compliance using active pinch grasp: The roles of force and work cues," *Perception Psychophys.*, vol. 57, no. 4, pp. 495–510, 1995.

[24] G. L. Beauregard, M. A. Srinivasan, and N. I. Durlach, "The manual resolution of viscosity and mass," in *ASME Dynamic Systems and Control Division*, vol. 1. New York, NY, USA: ASME, 1995, pp. 657–662.

[25] W. Fu, M. M. van Paassen, and M. Mulder, "On the relationship between the force JND and the stiffness JND in haptic perception," in *Proc. ACM Symp. Appl. Perception*, Cottbus, Germany, Sep. 2017, Art. no. 11.

[26] M. Khner, J. Wild, H. Bubb, K. Bengler, and J. Schneider, "Haptic perception of viscous friction of rotary switches," in *Proc. IEEE World Haptics Conf.*, Istanbul, Turkey, Jun. 2011, pp. 587–591.

[27] J. Schmidtler and M. Körber, "Human perception of inertial mass for joint human-robot object manipulation," *ACM Trans. Appl. Perception*, vol. 15, no. 3, 2018, Art. no. 15.

[28] E. M. Rank, T. Schauß, A. Peer, S. Hirche, and R. L. Klatzky, "Masking effects for damping JND," in *Proc. Int. Conf. Human Haptic Sens. Touch Enabled Comput. Appl.*, Tampere, Finland, Jun. 2012, pp. 145–150.

[29] W. Fu, A. Landman, M. M. van Paassen, and M. Mulder, "Modeling human difference threshold in perceiving mechanical properties from force," *IEEE Trans. Human–Mach. Syst.*, vol. 48, no. 4, pp. 359–368, Aug. 2018.

[30] W. Fu, M. M. van Paassen, and M. Mulder, "Modeling the coupled difference threshold of perceiving mass and stiffness from force," in *Proc. IEEE Int. Conf. Syst., Man, Cybern.*, Miyazaki, Japan, Oct. 2018, pp. 1427–1432.

[31] W. Fu, M. M. van Paassen, D. A. Abbink, and M. Mulder, "Framework for human haptic perception with delayed force feedback," *IEEE Trans. Human–Mach. Syst.*, vol. 49, no. 2, pp. 171–182, Apr. 2019.

[32] F. A. A. Kingdom and N. Prins, *Psychophysics: A Practical Introduction*. New York, NY, USA: Academic, 2016.

[33] K. van der El, D. M. Pool, H. J. Damveld, M. M. van Paassen, and M. Mulder, "An empirical human controller model for preview tracking tasks," *IEEE Trans. Cybern.*, vol. 46, no. 11, pp. 2609–2621, Nov. 2016.

[34] P. Arcara and C. Melchiorri, "Control schemes for teleoperation with time delay: A comparative study," *Robot. Auton. Syst.*, vol. 38, no. 1, pp. 49–64, 2002.

[35] M. M. van Paassen, "Biophysics in aircraft control: A model of the neuromuscular system of the pilot's arm," Ph.D. dissertation, Dept. Control Simulation, Faculty Aerospace Eng. Delft Univ. Technol., Delft, The Netherlands, 1994.

[36] C. Carello and M. Turvey, "Dynamic (effortful) touch," *Scholarpedia Touch.*, T. Prescott, E. Ahissar, and E. Izhikevich. Eds., Atlantis Press, Paris, Nov. 22, 2015, pp. 227–240, doi: 10.2991/978-94-6239-133-8_18.

[37] C. Carello and M. Turvey, "Useful dimensions of haptic perception: 50 years after the senses considered as perceptual systems," *Ecol. Psychol.*, vol. 29, no. 2, pp. 95–121, 2017.

[38] K. Shockley, C. Carello, and M. Turvey, "Metamers in the haptic perception of heaviness and moveableness," *Perception Psychophys.*, vol. 66, no. 5, pp. 731–742, 2004.

[39] D. Van Baelen, J. Ellerbroek, M. M. van Paassen, and M. Mulder, "Design of a haptic feedback system for flight envelope protection," in *Proc. AIAA Model. Simul. Tech. Conf.*, Kissimmee, FL, USA, Jan. 2018, Paper AIAA-2018-0117.

[40] S. de Stigter, M. Mulder, and M. M. van Paassen, "Design and evaluation of a haptic flight director," *J. Guid., Control, Dyn.*, vol. 30, no. 1, pp. 35–46, 2007.

[41] W. Fu, M. M. van Paassen, and M. Mulder, "Developing active manipulators in aircraft flight control," *J. Guid., Control, Dyn.*, vol. 42, pp. 1755–1767, 2019.